Published in final edited form as:
Neuroscience. 2007 May 11; 146(2): 713–729.

DISTINCT REGIONAL AND SUBCELLULAR LOCALIZATION OF ADENYLYL CYCLASES TYPE 1 AND 8 IN MOUSE BRAIN

Alana C. Conti[1], **James W. Maas Jr.**[1], **Lisa M. Muglia**[1], **Bhumy A. Dave**[1], **Sherri K. Vogt**[1], **Timothy T. Tran**[1], **Elizabeth J. Rayhel**[2], and **Louis J. Muglia**[1,*]

1 *Departments of Pediatrics, Molecular Biology and Pharmacology, Washington University School of Medicine, St. Louis, Missouri, 63110*

2 *Department of Biological and Physical Sciences, Fontbonne University, St. Louis, Missouri 63105*

Abstract

Adenylyl cyclases (ACs) convert ATP to cAMP and therefore, subserve multiple regulatory functions in the nervous system. AC1 and AC8 are the only cyclases stimulated by calcium and calmodulin, making them uniquely poised to regulate neuronal development and neuronal processes such as learning and memory. Here, we detail the production and application of a novel antibody against mouse AC1. Along with AC8 immunohistochemistry, these data reveal distinct and partially overlapping patterns of protein expression in brain during development and adulthood. AC1 protein increased in abundance in the neonatal hippocampus from postnatal day 7 to 14. By adulthood, abundant AC1 protein expression was observed in the mossy fiber tract in the hippocampus and the molecular layer in the cerebellum, with diffuse expression in the cortex and thalamus. AC8 protein levels were abundant during development, with diffuse and increasing expression in the hippocampus that intensified in the CA1/CA2 region by adulthood. AC8 expression was weak in the cerebellum at postnatal day 7 and decreased further by postnatal day 14. Analysis of synaptosome fractions from the adult brain demonstrated robust expression of AC1 in the postsynaptic density and extrasynaptic regions, while expression of AC8 was observed in the presynaptic active zone and extrasynaptic fractions. These findings were confirmed with localization of AC1 and/or AC8 with PSD-95, Tau, synaptophysin and MAP-2 expression throughout the brain. Together, these data provide insight into the functional roles of AC1 and AC8 as reflected by their distinct localization in cellular and subcellular compartments.

Keywords

cAMP; presynaptic; synaptosome; calcium; calmodulin

The ability of the brain to respond and process information dynamically is dependent on intercellular and intracellular neuronal signaling. Adenylyl cyclases (ACs), which generate cAMP, are critical to the integration of this signaling and are essential to processes such as

Address correspondence to: Louis J. Muglia, Departments of Pediatrics, Molecular Biology and Pharmacology, Washington University School of Medicine, Box 660 S. Euclid Ave, Campus Box 8208, St. Louis, Missouri 63110, Tel. 314 286-2847; Fax. 314 286-2893; Email: l_muglia@kids.wustl.edu

Section Editor- Dr. Werner Sieghart, Molecular Neuroscience

This work was supported by grants from the National Institutes of Health (AG18876, L.J.M., HD49305, A.C.C.) and the National Institute on Alcohol Abuse and Alcoholism (AA12957, L.J.M.)

learning and memory. Known AC isoforms share general structural organization as predicted by hydropathy and sequence analysis, including a short cytoplasmic amino terminus, two six-transmembrane domains, a 40-kD cytoplasmic loop and a cytoplasmic carboxy terminus of about 35 kD (Ferguson and Storm, 2004). Despite similarities in their structural composition, the ten identified mammalian AC isoforms differ in their functional characteristics (Cooper, 2003), reflecting the diversity among cAMP-dependent mechanisms. Roles of each AC are based partially on their regulatory properties, such as their degree of stimulation or inhibition by Ca^{2+}/calmodulin, $G\alpha_s$, or $G\beta\gamma$. AC1 and AC8 are the only two isoforms that are primarily stimulated by Ca^{2+} via calmodulin although some isoforms are sensitive to Ca^{2+} alone (Tang et al., 1991,Cali et al., 1994,Wong et al., 1999,Chern, 2000,Wang et al., 2003). The ability of AC1 and AC8 to be directly activated by Ca^{2+}/calmodulin imparts a unique function to these isoforms during neuronal development, a process that is critically controlled by calcium activity (Konur and Ghosh, 2005).

Further insight into the unique roles of the ACs is gained by examining their expression pattern and cellular localization. Within the neonatal brain, *in situ* hybridization analysis has revealed limited expression of AC8 mRNA in the cortex, CA1 region of the hippocampus, cerebellum, olfactory bulbs, hypothalamus, amygdala and basal ganglia (Nicol et al., 2005). In adulthood, expression of AC8 mRNA continued within the cerebellum, olfactory bulb, piriform and cerebral cortices, habenula, CA1 region of the hippocampus, and hypothalamus, with diffuse expression in the thalamus (Krupinski et al., 1992,Cali et al., 1994,Matsuoka et al., 1994,Muglia et al., 1999,Schaefer et al., 2000). The expression of AC8 in the hypothalamus is of particular importance, as AC8 is the only Ca^{2+}/calmodulin-stimulated cyclase in this brain region, suggesting a key role for AC8 in neuroendocrine activities, such as the stress response (Muglia et al., 1999,Schaefer et al., 2000). Detailed spatiotemporal localization of AC1 mRNA indicates widespread embryonic expression in several brain structures including the striatum, dorsal thalamus, trigeminal nerve nuclei, cerebellum, hippocampus, basolateral amygdala, and cortex (Villacres et al., 1995,Nicol et al., 2005). By adulthood, mRNA expression of AC1 is confined to the cerebellum, cortex, dentate gyrus and CA1 regions of the hippocampus, olfactory bulb, pineal gland, and various thalamic nuclei (Xia et al., 1991,Villacres et al., 1995,Tzavara et al., 1996,Matsuoka et al., 1997,Nicol et al., 2005). Notably, AC1 mRNA is expressed only in neurons making it uniquely positioned to regulate neuronal processes, including learning and memory (Xia et al., 1991,Xia et al., 1993).

Physiological processes involving synaptic plasticity, such as learning and memory formation, are effectively modeled by long-term potentiation (LTP). LTP can require both the increase of intracellular Ca^{2+} and the activation of downstream kinases, such as cAMP-dependent protein kinase A (PKA), making the production of cAMP by AC a pivotal step in neuroplastic activity. Studies evaluating the functional roles of AC1 and AC8 indicate that Ca^{2+}/calmodulin-stimulated adenylyl cyclase activity is required for both pre- and postsynaptic LTP (Villacres et al., 1998,Wong et al., 1999). Generation and analysis of AC1KO and AC8KO mice has shed important light on the many essential physiological functions these enzymes serve. For example, deletion of AC8 or AC1 in the mouse results in reduced hippocampal mossy fiber LTP (Villacres et al., 1998,Wang et al., 2003) in addition to disruption of cerebellar LTP observed in AC1KO mice (Storm et al., 1998). However these data do not distinguish between presynaptic or postsynaptic roles for AC1 or AC8. High expression of AC1 in the parallel fiber-Purkinje cell synapse in the cerebellum suggests a presynaptic role for AC1 (Storm et al., 1998), while disruption of LTP and long-term depression (LTD) at the thalamocortical synapse in AC1 "*barrelless*" mutant mice is demonstrated to be an AC1-dependent postsynaptic phenomenon (Lu et al., 2003). Recent evidence from *barrelless* mice has likewise implicated AC1 in the presynaptic regulation of neurotransmission (Lu et al., 2006). Although limited, data regarding the subcellular distribution of AC8 reveals its co-localization with both

presynaptic and postsynaptic proteins upon transfection into cortical and hippocampal neurons *in vitro* (Wang et al., 2003).

Despite our ability to localize AC1 and AC8 mRNA, to date, there is little information on AC1 and AC8 protein distribution in the mouse brain. Although detection of AC1 has proven technically challenging in the rodent, AC1 has been demonstrated in limited regions of the monkey brain, including the mossy fiber pathway and the molecular layers of the dentate gyrus and CA1-3 regions of the hippocampus (Kumar et al., 2001). Further analysis of AC1 protein has been limited due to the lack of specific and reliable antibodies. In this report, we detailed methods for sensitive and specific detection of AC1 and AC8 in the mouse in order to examine protein distribution throughout the adult and neonatal brain. The overlapping regional expression suggests redundant functions of AC1 and AC8. However, we provide evidence that AC1 and AC8 are only partially localized to the same cell populations, suggestive of differential functions. In addition, we have isolated synaptosome fractions from the adult mouse brain to localize AC1 and AC8 differentially within the pre-, post- and extrasynaptic subcellular compartments and have confirmed these results using immunofluorescent co-localization. These data are the first to provide insight into the roles of AC1 and AC8 proteins as reflected by their distinct localization in neuronal compartments *in vivo*.

EXPERIMENTAL PROCEDURES

Animal Husbandry

All mice were backcrossed at least ten generations to wild type C57BL/6 (WT) mice from The Jackson laboratory (Bar Harbor, ME). To generate mice for these studies, we used progeny of homozygous mutants (AC1KO, AC8KO, AC1/AC8KO) and WT mice bred in our colony. Mice were maintained on a 12 h light/dark schedule with *ad libitum* access to food and water. All mouse protocols were in accordance with the National Institutes of Health guidelines and were approved by the Animal Care and Use Committee of Washington University School of Medicine.

Generation of AC1 Antibody

A thioredoxin-tagged AC1 recombinant protein of 65 amino acids (#1054-1118) was derived from the C2b region of the mouse AC1 protein, which was divergent from amino acid sequences of the other AC isoforms. This recombinant protein was cloned and expressed using the pET E. coli expression system (pET32a, Novagen) and isolated for injection into rabbits using a standard 63-day injection protocol (Alpha Diagnostics). Injections were administered at 15-day intervals at 2–4 subcutaneous sites and 1 intramuscular site in complete Freund's adjuvant for the first injection with all subsequent injections given in incomplete adjuvant. This protein resulted in high-titer serum that was affinity purified by Amino-link coupling of the purified antigen to Sepharose 4-B (Alpha Diagnostics).

Protein Immunoblot Analysis

Seven day-, ten day-, fourteen day- or ten week old WT, AC8KO and AC1KO male mice were killed by CO_2 inhalation and the brains rapidly removed. Subregions were dissected on ice, snap frozen in liquid nitrogen and stored at −80°C. Frozen hippocampal, cerebellar and cortical tissues were homogenized in buffer A (20 mM Tris-HCl (pH 7.4), 2 mM $MgCl_2$, 1 mM ETDA, 0.5 mM DTT, 5 μg/ml leupeptin, and 0.5 mM phenylmethanesulfonyl fluoride (PMSF)), at 4° C. Homogenates were centrifuged at 600 × g for 2 min, and the resulting membrane-enriched supernatants centrifuged at 30,000 × g for 20 min. Protein concentration was determined by the BCA assay (Pierce Biotechnology). For AC1 detection in adult brain, 80 μg of membrane extract from each region was separated by 4–12% SDS-PAGE, transferred to nitrocellulose membrane using a semi-dry preparation (15V for 50 min). The membrane was blocked in 5%

nonfat dry milk/Tween 20-Tris-buffered saline (0.1% Tween-20 in 26 mM Tris-HCl [pH 8.0], 0.9% NaCl) for 1 hr at room temperature followed by incubation overnight at 4°C with rabbit anti-AC1 antibody (1:500 in blocking buffer). For AC8 detection in adult brain, 20 μg of membrane extract from each region was separated by 4–12% SDS-PAGE, transferred to nitrocellulose membrane and immunoblotted with goat anti-AC8 antibody (1:500, Santa Cruz Biotechnology) as described for anti-AC1 antibody. For neonatal AC1 and AC8 expression, 30 μg of membrane extract from each region (n=3/timepoint) was separated by 4–12% SDS-PAGE, transferred to nitrocellulose membrane and immunoblotted with antibodies against AC1 or AC8 as described. Equal protein loading conditions were verified by immunodetection for mouse anti-binding protein (BiP) in all samples except neonatal cerebellar samples. Signals were detected using anti-rabbit, anti-goat, or anti-mouse HRP-conjugated secondary antibodies, as appropriate, and visualized using chemiluminescence (SuperSignal WestDura; Pierce Biotechnology). Densitometric analysis was performed using NIH Image Software. Due to increases in BiP protein during development in the cerebellum, neonatal cerebellar signals for AC1 and AC8 were normalized to their respective signals from P7 samples. Expression of AC1 and AC8 from neonatal hippocampal and cortical samples were normalized to BiP expression. Student's t-test was performed using GraphPad Prism 4.0 software (Hearne Scientific Software).

Immunohistochemical Analysis

Seven day-, fourteen day- or ten week old WT, AC8KO, AC1KO and AC8/AC1KO (DKO) male mice were anesthetized and transcardially perfused with 4% paraformaldehyde. After perfusion brains were removed, postfixed for 24 hr (adult) or 72 hr (neonatal) in 4% paraformaldehyde, cryoprotected in 30% sucrose and frozen at −80°C until use. Frozen tissues were cut into 40 μm (adult) or 55 μm (neonatal) slices and stored free-floating in 1X PBS/0.1% NaN_3 at 4°C. For AC1 analysis, sections from adult or neonatal mice were quenched of endogenous peroxidases with 0.3%H_2O_2/0.75% Triton X-100 for 1 hr, washed in 1X PBS and blocked with 1% normal goat serum/10% fish gel/0.6% nonfat dry milk (blocking solution A) for 1 hr. Sections were incubated in rabbit anti-AC1 antibody (1:400 in blocking solution A) overnight at 4°C with continued incubation at room temperature for 4 hr the next day. Sections were then incubated in blocking solution A for 1 hr. Following treatment with biotinylated goat anti-rabbit secondary antibody (Vector Labs) at 1:800 for 1 hr, sections were blocked again as described. Biotin was detected with an ABC Kit (Vector Labs) and visualized using TSA+ Cyanine 3 (Tyramide amplification) kit (1:1000, Perkin Elmer) for 3 min. Sections were slide-mounted using Vectashield mounting medium containing DAPI (Vector Labs) counterstain for visualization of anatomical landmarks. For AC8 analysis, sections from adult or neonatal mice were quenched of endogenous peroxidases with 0.3%H_2O_2/0.75% Triton X-100 for 1 hr, washed in 1X PBS and blocked with 1% normal rabbit serum/10% fish gel/0.6% nonfat dry milk (blocking solution B) for 1 hr. Sections were incubated in goat anti-AC8 antibody (1:400, Santa Cruz Biotechnology, in blocking solution B) overnight at 4°C followed by incubation in blocking solution B for 1 hr. Following treatment with biotinylated rabbit anti-goat secondary antibody (Vector Labs) at 1:800 for 1 hr sections were blocked again as described. Biotin was detected and sections were slide-mounted as described for AC1 analysis. All images were obtained using matched settings between genotypes on an Olympus BX60 fluorescent microscope equipped with Axiovision software. Images were prepared using Adobe Photoshop Software.

Synaptosome Isolation

Isolation of synaptosome fractions was performed according to the methods detailed by Phillips et al (Phillips et al., 2001). *Synaptosome isolation*: Individual forebrain regions (containing hippocampus and cortex) were freshly isolated from WT, AC1KO and AC8KO male mice killed by CO_2 inhalation. All subsequent steps were performed at 4°C. Tissues were

homogenized using a Teflon/glass homogenizer in 0.32 M sucrose, 0.1 mM $CaCl_2$, 1 mM $MgCl_2$, 40 μg/ml PMSF, 1:200 Sigma protease inhibitor cocktail using 3 ml/gm wet weight of tissue. Next, 2 M sucrose and 0.1 M $CaCl_2$ were added to bring homogenates to a final concentration of 1.25 M sucrose/0.1 mM $CaCl_2$. Samples were divided into 2–10 mL Oak Ridge centrifuge tubes, layered with 2.8 ml of 1 M sucrose/0.1 M $CaCl_2$ followed by 1.4 mL of homogenization buffer (not containing protease inhibitors). Samples were centrifuged 1.5 hr at 100,000 × g (maximum centrifugal force). Synaptosomes were isolated from the 1.25 M/1 M sucrose interface. *Synaptosome fractionation*: Synaptosomes were combined with equal volumes of 2X solubilization buffer (40 mM Tris, pH 6.0, 2% Triton X-100 and 1 mM PMSF). Following agitation for 30 min, samples were centrifuged at 40,000 × g for 30 min. Four milliliters of the resulting supernatant were precipitated with 24 ml of –20°C acetone and centrifuged at 18,000 × g for 30 min at −15°C. The pellet resulting from the acetone precipitation represents the extrasynaptic fraction and was resuspended in 400 μL 5% SDS. For pre- and postsynaptic junctions, the pellet resulting from centrifugation at 40,000 × g spin was washed with pH 6.0 solubilization buffer (20 mM Tris, pH 6.0, 1% Triton X-100) and resuspended in 10 volumes of pH 8.0 solubilization buffer (20mM Tris, pH 8.0, 1% Triton X-100, 40 μg/ml PMSF, 1:200 Sigma protease inhibitors). Following 30 min agitation on ice, fractions were centrifuged at 40,000 × g for 30 min. The resulting supernatant represents the presynaptic active zone (PAZ) which was acetone precipitated as above and resuspended in 5% SDS. The remaining pellet resulting from centrifugation of the pH 8.0 solubilization fraction represents the postsynaptic density (PSD) fraction and was resuspended in 5% SDS directly. Protein concentrations were determined using the BCA assay (Pierce Biotechnology).

Synaptosome fractions from WT, AC1KO and AC8KO were separated by 4–12% SDS-PAGE, transferred to nitrocellulose membrane and immunoblotted with polyclonal rabbit anti-AC1 antibody (60 μg per lane, 1:500), polyclonal anti-AC8 antibody (Santa Cruz Biotechnology, 20 μg per lane, 1:500), polyclonal anti-phosphoserine NR2B antibody (Upstate Cell Signal, 60 μg per lane, 1:500), monoclonal anti-PSD95 antibody (Affinity Bioreagents, 20 μg per lane, 1:4000), monoclonal anti-synaptophysin antibody (Chemicon, 4 μg per lane, 1:2000), or polyclonal anti-SNAP-25 antibody (Chemicon, 4 μg per lane, 1:2000). Signals were detected using appropriate HRP-conjugated secondary antibodies and visualized using chemiluminescence (SuperSignal WestDura; Pierce Biotechnology).

Confocal microscopy

Age-matched adult C57BL/6 (WT), AC1/AC8KO (DKO) or AC8KO male mice were perfused, postfixed and cryoprotected as described. Frozen tissue was cut into 35 μm slices and stored free-floating in 1X PBS at 4°C. Primary antibodies used for co-localization of AC1 and AC8 included: mouse anti-MAP-2 (1:400, Chemicon), mouse anti-Tau (1:400, Chemicon) and mouse anti-PSD-95 (1:300, Affinity BioReagents). These were applied prior to AC1 or AC8 staining when co-localizing. Secondary antibodies included: Alexafluor 647-conjugated donkey anti-mouse (1:800, Molecular Probes) for Tau, synaptophysin, and PSD-95 and Cy5-conjugated donkey anti-mouse with minimal cross reactivity (1:500, Jackson ImmunoResearch) for MAP-2. Sections were quenched of endogenous peroxidases with 0.3% H2O2/0.3% Triton X-100 in 1X PBS (for MAP-2: 0.75% Triton X-100) for 1 hr, washed with 1X PBS, then blocked with 1.7% normal donkey serum (NDS)/1.7% fish gel in 1X PBS (5% fish gel/4% NDS for MAP-2) for 45 min. PSD-95 and Tau antibodies were diluted in their respective blocking solution, while the MAP-2 antibody was diluted in 2% fish gel/4% NDS in 1X PBS. Sections were incubated with primary antibodies overnight at 4°C. Sections were washed with 1X PBS, incubated in blocking solution as above, then exposed to secondary antibodies (diluted as the primary antibodies) for 1 hr. After washing with 1X PBS sections were returned into the appropriate blocking solution for AC1 or AC8 staining. Control sections

included: the above primary antibodies with no AC antibody added and incubation in secondary antibodies alone.

The AC1 and AC8 antibodies used were the same as described above. Rabbit anti-AC1 antibody was applied at 1:400 and goat anti-AC8 antibody was used at 1:1000. Secondary antibodies included: biotinylated donkey anti-rabbit with minimal cross reactivity (1:500, Jackson ImmunoResearch) for AC1 and biotinylated donkey anti-goat with minimal cross reactivity (1:1000, Jackson ImmunoResearch) for AC8. Sections for AC1 analysis were blocked in 10% fish gel/1.7% NDS/0.3% nonfat dry milk in 1X PBS for 45 min then incubated overnight with AC1 in antibody diluent (2%fish gel/0.8% NDS/0.3% nonfat dry milk in 1X PBS) at 4°C. AC1 incubation continued at room temperature for 4 hr the next day. Sections were washed and blocked as described above then incubated with secondary antibody in the antibody diluent for 1 hr. Biotin was detected as described above. Sections were slide-mounted with propyl gallate mounting medium. A similar protocol was followed for co-localization with AC8, with the following differences: blocking solution: 10% fish gel/2.2% NDS/0.2% nonfat dry milk, antibody diluent: 2% fish gel/1.3%NDS/0.2% nonfat dry milk and no incubation with primary antibody was performed at room temperature.

Confocal images were acquired using matched settings between genotypes on an Olympus BX61WI microscope equipped with Fluoview 500 software. A 543 nm green He-Ne laser was used to detect Cy3 and a 633 nm red He-Ne laser was used to detect Cy5 and Alexafluor 647 at z-step thicknesses ranging from 0.03–0.05 μm. Images (1024 × 1024 pixels) were prepared using Adobe Photoshop Software.

RESULTS

An AC1 antibody suitable for use in protein immunoblot and immunohistochemical applications was generated against a thioredoxin-tagged fragment of AC1 (amino acid #1054–1118, accession #NP_033752) unique to the C2b catalytic region of the AC1 protein. The peptide antigen used to generate antibodies against AC8 (#sc-1967, Santa Cruz Biotechnology, Inc.) is an amino acid sequence that maps within the carboxy terminal region (amino acid #1170–1248).

In order to examine the temporal and regional protein expression of AC1 and AC8, protein immunoblots were performed. Membrane-enriched protein extracts from cortex, hippocampus and cerebellum of adult and neonatal mice were subjected to SDS-PAGE and immunoblotted with anti-AC1 or anti-AC8 antibodies. In adult mice, AC1 protein was detected in all regions examined in WT, but not AC1KO mice as evidenced by a prominent immunoreactive band at ~123 kD in all WT samples, which is the predicted size of the AC1 protein (Fig. 1*A*). In the adult brain, relative levels of AC1 protein were highest in the cerebellum with the lowest expression observed in the hippocampus. Similar to AC1, adult AC8 expression was detected in WT cortex, hippocampus and cerebellum as a ~135 kD band, which was absent in AC8KO samples (Fig. 1*B*).

Protein immunoblot analysis of neonatal AC1 expression revealed progressively increasing AC1 protein expression from P7 to P14 in the hippocampus (Fig. 2*A*, *D*). Although detectable at P7, AC1 hippocampal expression significantly increased (nearly 4-fold) by P14 (Fig. 2*D*, *, $p < 0.05$). Cortical expression of AC1 gradually increased, although not significantly, from P7 to P14 (Fig. 2*B*, *E*). Robust expression of AC1 was observed in the cerebellum at P7 (Fig. 2*C*). AC1 protein levels remained consistent through P10, with a trend towards increased expression by P14 (Fig. 2*F*).

In the neonatal hippocampus, levels of AC8 protein significantly increased (nearly 5-fold) from P7 to P14, (Fig. 2*A*, *D*, *, $p < 0.05$). Also similar to AC1 in the neonatal cortex, AC8 levels

showed a trend towards increased expression from P7 to P10, although values remained unchanged by P14 (Fig. 2*B*, *E*). In contrast to other regions examined, AC8 levels in the neonatal cerebellum significantly decreased after P7, with significantly lower levels expressed by P14 (Fig. 2*C, F*, *, $p < 0.05$*)*.

Protein immunoblot analysis of AC1 and AC8 in P14 and adult tissues, revealed a significant reduction of AC1 in the hippocampus and cortex of wild type mice from P14 to adulthood (Fig. 3*A, B, D*, *, $p < 0.05$). This was not observed in the cerebellum, where AC1 expression was unchanged with age after P14 (Fig. 3*C*, *D*). Similar results were observed with AC8 immunoreactivity in that a significant reduction in AC8 levels was detected from P14 to adulthood (Fig. 3*A*, *E*) in the hippocampus, while no significant changes in AC8 expression were detected after P14 in the cortex or cerebellum (Fig. 3*B*, *C*, *E*).

In order to determine the differential cellular distribution of AC1 and AC8, we performed immunohistochemistry. As predicted by mRNA expression patterns in the adult brain, the most intense AC1 immunoreactivity in the adult brain was localized to the mossy fiber projections from the dentate hilus region extending to the stratum lucidum of the CA3 region of the hippocampus (Fig. 4*A*, Fig. 5*A*). AC1 was also weakly detected in the dendritic arbors of the dentate gyrus (Fig. 5*A*). AC1 was widely distributed, although in lesser amounts, in the mature cortex and thalamus, without localization to a particular cell layer or nucleus (Fig. 4*A*, Fig. 5*B*). Abundant staining was observed in the molecular layer of the adult cerebellum, which contains parallel fibers that extend from cerebellar granule cells (Fig. 5*C*). In comparing the adult hippocampal distribution of AC1 and AC8, while the majority of AC1 was expressed in the mossy fiber tract, AC8 localized to dendritic arbors in the oriens, molecular layer and stratum radiatum of the mature CA1/CA2 region (Fig. 4*B*, Fig. 6*B*). In agreement with mRNA patterns, robust AC8 expression was also observed in the habenula, retrosplenial cortex and thalamus with positive, but more diffuse expression, in the intermediate layers of the cerebral cortex and the molecular layer of the cerebellum in the adult brain (Fig. 4*B*, Fig. 6*A*, *C*, *D*). Significant staining was also observed in the mature olfactory bulb (data not shown).

In the developing hippocampus, AC1 expression is notably diffuse at P7 (Fig. 7*A*). By P14, the pattern of AC1 protein expression resembles that observed in the adult hippocampus, with robust expression localized to the dendritic arbors of the dentate gyrus and the mossy fiber projections (Fig. 7*B*). As in the adult brain, expression of AC1 in the neonatal cortex was widespread and this pattern was maintained throughout development to P14 (Fig. 7*C*, *D*). Thalamic AC1 expression intensified throughout development resulting in diffuse expression across several nuclei by P14, a pattern that persisted to adulthood (Fig. 7*E*, *F*).

Neonatal hippocampal analysis revealed generalized AC8 staining at P7, which localized to the CA1/CA2 regions of the hippocampus by P14 (Fig. 8*A*, *B*). Similar distribution of AC8 protein was observed across cortical layers with slightly increased expression in the deeper cortical layers at P7 progressing to the intermediate layers by P14 (Fig. 8*C*, *D*). Throughout development, thalamic expression was widespread across various nuclei from P7 to P14, including dorsal and ventral thalamic nuclei as well as ventromedial and mediolateral nuclei (Fig. 8*E*, *F*). As in the adult, robust AC8 expression was observed in the habenula at both P7 and P14 (Fig. 8*E*, *F*).

Biochemical fractionation techniques for synaptosomes were used to assess the subcellular distribution of AC1 and AC8 within forebrain regions. This fractionation yields proteins enriched in the postsynaptic density (PSD), presynaptic active zone (PAZ) and a fraction designated “extrasynaptic” which contains both pre- and postsynaptic regions that are not localized to the PSD or PAZ (Phillips et al., 2001). Synaptosome analysis revealed that AC1 and AC8 have distinct patterns of subcellular distribution (Fig. 9). While both AC1 and AC8

immunoreactivity was found in the extrasynaptic fraction, AC1 localized strongly to the PSD with minimal expression in the PAZ. In contrast, AC8 was expressed more robustly in the PAZ with only slight expression in the PSD. The weak synaptophysin signal observed in the PAZ fraction could be a result of incomplete separation of the pH6 soluble (extrasynaptic) and insoluble fractions (PAZ), which may bring to question the presence of AC8 in the PAZ. However co-localization of AC8 with synaptophysin using immunofluorescent methods supports the presence of AC8 in extrasynaptic membrane regions and in the PAZ (see results below). Specificity of the fractionation procedure was confirmed with immunodetection of pre-, post-, and extrasynaptic markers, such as phosphoserine NR2B (postsynaptic), PSD-95 (postsynaptic), synaptophysin (extrasynaptic) and SNAP-25 (pre- and extrasynaptic).

To provide subcellular localization and confirmation of synaptosomal fractionation results, immunohistochemical co-localization of AC1 or AC8 was performed with protein markers and methods that have been successfully utilized to distinguish pre- and postsynaptic sites (Serpinskaya et al., 1999,Fukaya and Watanabe, 2000,Lachamp et al., 2005,Sindreu et al., 2007). Co-expression of AC1 and PSD-95 was observed within multiple structures of the hippocampus (Fig. 10), including the mossy fibers extending from the dentate hilus, the mossy fiber/CA3 pyramidal cell junction and the dendritic arbors of dentate granule cells (Fig. 10*B*). Additional co-localization of AC1 and PSD-95 was detected in the CA1 region (data not shown). These results support those of the synaptosomal fractionation experiments, in which robust AC1 expression was observed in the postsynaptic density fraction. In addition to the PSD, strong expression of AC1 was detected in the extrasynaptic synaptosome fraction. Therefore, co-localization of AC1 with Tau, the axonal microtubule protein, was performed (Fig. 11). Co-expression of AC1 with Tau was observed in the hippocampus, suggesting that AC1 expression is also axonal in this region, validating the presence of AC1 in the extrasynaptic synaptosome fraction. Within the hippocampus, AC1 was observed to co-localize with Tau in both the proximal mossy fiber pathway and the mossy fiber/CA3 pyramidal cell junction (Fig. 11*B*).

Immunoblot analysis of synaptosome fractions demonstrated that AC8 expression was primarily localized to the extrasynaptic fraction and the presynaptic active zone. These data are supported by the co-expression of AC8 with the dendritic marker, MAP-2 (microtubule-associated protein-2), Tau (Fig. 12) and synaptophysin (data not shown). Intense co-localization of AC8 and Tau was observed the cingulate cortex (Fig. 12*A*) and the thalamus (data not shown), indicating the presence of AC8 in axonal/presynaptic regions. Dendritic expression of AC8 is supported by the co-localization of AC8 with MAP-2 in the cingulate cortex (Fig. 12*B*). In this region, as well as in the hippocampus, hypothalamus, and other cortical layers (data not shown) dendrites demonstrated both independent and co-expression of AC8 and MAP-2. Co-expression of synaptophysin and AC8 was used to examine the presence of AC8 in presynaptic regions (data not shown). Strong co-localization of AC8 and synaptophysin was observed in both the cingulate cortex and the thalamus. As synaptophysin is associated with synaptic vesicles concentrated in the axon terminal and the PAZ, its immunohistochemical co-localization with AC8 suggests that AC8 is located on presynaptic membranes adjacent to synaptic vesicles and the PAZ.

DISCUSSION

In this study, we demonstrate the specificity and versatility of a novel antibody that recognizes mouse AC1, making it a valuable tool for understanding AC1 regulation and function. In conjunction with commercially available AC8 antibodies, our results demonstrate partially overlapping and distinct localization patterns of AC1 and AC8 proteins at the regional and subcellular levels. The analysis of AC1 and AC8 protein levels through the use of protein immunoblots and immunohistochemistry have yielded consistent and correlated results. The

overall patterns of AC1 and AC8 distribution in the brain are in agreement with previously published reports of their mRNA expression (Xia et al., 1991,Matsuoka et al., 1992,Xia et al., 1993,Cali et al., 1994,Matsuoka et al., 1994,Villacres et al., 1995,Tzavara et al., 1996,Muglia et al., 1999,Schaefer et al., 2000,Nicol et al., 2005) and calcium-stimulated cyclase activity (Villacres et al., 1995,Villacres et al., 1998,Wong et al., 1999). AC1 and AC8 are robustly expressed in the cortex, hippocampus and cerebellum in both early postnatal development and adulthood. Postnatal hippocampal expression was greater for AC1 and AC8 compared to the adult, underscoring their importance during developmental processes. In addition, their dynamic expression patterns throughout development reflect different temporal requirements of cAMP production. Hippocampal, thalamic and cortical AC1 expression appeared more widely distributed during development than that of AC8. These data support the observation of significant disruption of thalamocortical synapse development and barrel formation in the spontaneous AC1 mutant (*barrelless*) mouse (Lu et al., 2003). In contrast, there are no overt developmental abnormalities reported to date in AC8KO mice, suggesting a more conservative role of AC8 in neuronal development.

Neonatal expression of AC1 and AC8 exhibited regional variation. In the hippocampus, both AC1 and AC8 demonstrated significant increases from P7 to P14. This pattern varied from the cortex in which both AC1 and AC8 exhibited a modest, but not significant, increase by P10 that was maintained through P14. The most extreme differences were observed in the cerebellum, where AC1 was robustly expressed by P7 and increased only slightly with time, while AC8 was only weakly expressed by P7 and declined significantly by P14. These patterns of expression correlate well with reports of Ca^{2+}/calmodulin-stimulated AC activity (which represent both AC1 and AC8 activity) in the neonatal brain (Villacres et al., 1995,Matsuoka et al., 1997). Ca^{2+}/calmodulin-stimulated activity was reported to peak sharply around P14 in the hippocampus and cerebellum during the postnatal period. Similarly, there was progressively increasing Ca^{2+}/calmodulin-stimulated activity from P7 to P14 in the cortex.

The robust protein localization of AC1 observed in the mossy fiber pathway of the hippocampus is in agreement with previous data implicating AC1 in mossy fiber LTP (Villacres et al., 1998) and reports of AC1 as the primary Ca^{2+}/calmodulin-stimulated AC in the CA3 hippocampal region (Wang et al., 2003). Mossy fiber/CA3 LTP is a presynaptic event that is independent of NMDA receptors but may require elevations in presynaptic intracellular calcium (Zalutsky and Nicoll, 1990). AC1 is hypothesized to couple calcium to the cAMP signal transduction system leading to increased PKA activity. This hypothesis is based on the significant reduction of mossy fiber LTP in AC1KO mice (Villacres et al., 1998). Recent evidence from *barrelless* mice also suggests a presynaptic role for AC1 in neurotransmission (Lu et al., 2006). Specifically, AC1 deficiency in these mice results in impaired phosphorylation of Rab3-interacting molecules, which are active zone proteins essential to neurotransmission. Although AC1 immunoreactivity was faintly detected in the presynaptic active zone fraction of the synaptosome, presynaptic membranes away from the PAZ are represented in the extrasynaptic fraction. We hypothesize that the primary presynaptic actions of AC1 take place in this extrasynaptic region, outside of the immediate PAZ. This is supported by the co-localization of AC1 with Tau in hippocampal regions. Reports of AC1's increased sensitivity to calcium compared to that of AC8 is consistent with its presence in extrasynaptic membranes (Villacres et al., 1995). That is, despite its localization away from the PAZ, the increased calcium sensitivity of AC1 provides a mechanism by which it can respond to lower levels of calcium that may be present outside the immediate PAZ.

In addition to its hypothesized function as a presynaptic modulator, data has emerged to demonstrate a postsynaptic role for AC1. For example, AC1 has been shown to regulate postsynaptic plasticity underlying thalamocortical synapse formation. Calcium influx through NMDA receptors is necessary for thalamocortical synaptic plasticity (Crair and Malenka,

1995,Feldman et al., 1998,Lu et al., 2001). The role of AC1 is to link postsynaptic calcium influx with PKA activation that is required for AMPA receptor regulation, a critical step in the formation of synaptic strength (Lu et al., 2003). The functional importance of postsynaptic AC1 is clearly demonstrated in mice with spontaneous deletion of AC1 (*barrelless*), which show defective barrel mapping in the somatosensory cortex (Welker et al., 1996). Our data demonstrating abundant AC1 immunoreactivity in synaptosomal postsynaptic density fractions and the co-expression of AC1 with PSD-95 support this proposed role for AC1 in postsynaptic activity.

While AC1 and AC8 have been hypothesized to serve compensatory functions, their distinct subcellular localization suggests different roles of these cyclases. In contrast to AC1, which was robustly expressed in the extrasynaptic fraction and the PSD, AC8 was primarily expressed in the extrasynaptic fraction and the PAZ. Our subcellular localization of AC8 to the PAZ and the co-localization of AC8 with the presynaptic marker synaptophysin, are in agreement with *in vitro* studies in which AC8KO mice have demonstrated impaired mossy fiber/CA3 LTP, a presynaptic process (Wang et al., 2003). Additional *in vitro* studies from Wang and colleagues co-localized hemagglutinin-tagged AC8 with both presynaptic proteins, such as synapsin, and postsynaptic proteins, such as PSD-95 (Wang et al., 2003). Although little AC8 was detected in the PSD, the extrasynaptic fraction comprises membranes from both pre-and postsynaptic cells and would account for the co-localization of AC8 with these postsynaptic proteins. This is supported by the co-localization of AC8 and the dendritic marker, MAP-2. Co-expression of AC8 and Tau suggests a role for AC8 in axonal regions proximal to the axon terminal, which are present in the extrasynaptic fraction of the synaptosome, while co-expression of AC8 and synaptophysin suggests a role for AC8 within terminal regions, including the presynaptic membranes adjacent to synaptic vesicles. While we have employed measures to optimize resolution of pre- and postsynaptic components of the synapse, the submicron proximity of these subcellular regions limits the certainty with which AC1 and AC8 can be assigned to these compartments. However, together with the biochemical fractionation methods, confidence is increased in these subcellular assignments.

Here we have utilized a novel antibody against mouse AC1, as well as available antibodies against AC8, to describe the protein distribution of these cyclases throughout development and in the adult brain. The dynamic and discrete expression patterns of both AC1 and AC8 during development and adulthood suggest the independent regulation of these cyclases. Additionally, the localization of AC1 and AC8 to unique subcellular fractions further underscores their complementary, but independent roles. These tools and techniques will prove useful in identifying mechanisms of AC1 and AC8 action as well as their interaction with proximal downstream targets in the synapse.

References

Cali JJ, Zwaagstra JC, Mons N, Cooper DM, Krupinski J. Type VIII adenylyl cyclase. A Ca2+/calmodulin-stimulated enzyme expressed in discrete regions of rat brain. J Biol Chem 1994;269:12190–12195. [PubMed: 8163524]

Chern Y. Regulation of adenylyl cyclase in the central nervous system. Cell Signal 2000;12:195–204. [PubMed: 10781926]

Cooper DM. Regulation and organization of adenylyl cyclases and cAMP. Biochem J 2003;375:517–529. [PubMed: 12940771]

Crair MC, Malenka RC. A critical period for long-term potentiation at thalamocortical synapses. Nature 1995;375:325–328. [PubMed: 7753197]

Feldman DE, Nicoll RA, Malenka RC, Isaac JT. Long-term depression at thalamocortical synapses in developing rat somatosensory cortex. Neuron 1998;21:347–357. [PubMed: 9728916]

Ferguson GD, Storm DR. Why calcium-stimulated adenylyl cyclases? Physiology (Bethesda) 2004;19:271–276. [PubMed: 15381755]

Fukaya M, Watanabe M. Improved immunohistochemical detection of postsynaptically located PSD-95/SAP90 protein family by protease section pretreatment: a study in the adult mouse brain. J Comp Neurol 2000;426:572–586. [PubMed: 11027400]

Konur S, Ghosh A. Calcium signaling and the control of dendritic development. Neuron 2005;46:401–405. [PubMed: 15882639]

Krupinski J, Lehman TC, Frankenfield CD, Zwaagstra JC, Watson PA. Molecular diversity in the adenylyl cyclase family. Evidence for eight forms of the enzyme and cloning of type VI. J Biol Chem 1992;267:24858–24862. [PubMed: 1332969]

Kumar PA, Baker LP, Storm DR, Bowden DM. Expression of type I adenylyl cyclase in intrinsic pathways of the hippocampal formation of the macaque (Macaca nemestrina). Neurosci Lett 2001;299:181–184. [PubMed: 11165765]

Lachamp P, Balland B, Tell F, Baude A, Strube C, Crest M, Kessler JP. Early expression of AMPA receptors and lack of NMDA receptors in developing rat climbing fibre synapses. J Physiol 2005;564:751–763. [PubMed: 15731186]

Lu HC, Butts DA, Kaeser PS, She WC, Janz R, Crair MC. Role of efficient neurotransmitter release in barrel map development. J Neurosci 2006;26:2692–2703. [PubMed: 16525048]

Lu HC, Gonzalez E, Crair MC. Barrel cortex critical period plasticity is independent of changes in NMDA receptor subunit composition. Neuron 2001;32:619–634. [PubMed: 11719203]

Lu HC, She WC, Plas DT, Neumann PE, Janz R, Crair MC. Adenylyl cyclase I regulates AMPA receptor trafficking during mouse cortical 'barrel' map development. Nat Neurosci 2003;6:939–947. [PubMed: 12897788]

Matsuoka I, Giuili G, Poyard M, Stengel D, Parma J, Guellaen G, Hanoune J. Localization of adenylyl and guanylyl cyclase in rat brain by in situ hybridization: comparison with calmodulin mRNA distribution. J Neurosci 1992;12:3350–3360. [PubMed: 1356144]

Matsuoka I, Maldonado R, Defer N, Noel F, Hanoune J, Roques BP. Chronic morphine administration causes region-specific increase of brain type VIII adenylyl cyclase mRNA. Eur J Pharmacol 1994;268:215–221. [PubMed: 7957643]

Matsuoka I, Suzuki Y, Defer N, Nakanishi H, Hanoune J. Differential expression of type I, II, and V adenylyl cyclase gene in the postnatal developing rat brain. J Neurochem 1997;68:498–506. [PubMed: 9003034]

Muglia LM, Schaefer ML, Vogt SK, Gurtner G, Imamura A, Muglia LJ. The 5'-flanking region of the mouse adenylyl cyclase type VIII gene imparts tissue-specific expression in transgenic mice. J Neurosci 1999;19:2051–2058. [PubMed: 10066258]

Nicol X, Muzerelle A, Bachy I, Ravary A, Gaspar P. Spatiotemporal localization of the calcium-stimulated adenylate cyclases, AC1 and AC8, during mouse brain development. J Comp Neurol 2005;486:281–294. [PubMed: 15844169]

Phillips GR, Huang JK, Wang Y, Tanaka H, Shapiro L, Zhang W, Shan WS, Arndt K, Frank M, Gordon RE, Gawinowicz MA, Zhao Y, Colman DR. The presynaptic particle web: ultrastructure, composition, dissolution, and reconstitution. Neuron 2001;32:63–77. [PubMed: 11604139]

Schaefer ML, Wong ST, Wozniak DF, Muglia LM, Liauw JA, Zhuo M, Nardi A, Hartman RE, Vogt SK, Luedke CE, Storm DR, Muglia LJ. Altered stress-induced anxiety in adenylyl cyclase type VIII-deficient mice. J Neurosci 2000;20:4809–4820. [PubMed: 10864938]

Serpinskaya AS, Feng G, Sanes JR, Craig AM. Synapse formation by hippocampal neurons from agrin-deficient mice. Dev Bio 1999;205:65–78. [PubMed: 9882498]

Sindreu CB, Scheiner ZS, Storm DR. Ca^{2+}-stimulated adenylyl cyclases regulate ERK-dependent activation of MSK1 during fear conditioning. Neuron 2007;53:79–89. [PubMed: 17196532]

Storm DR, Hansel C, Hacker B, Parent A, Linden DJ. Impaired cerebellar long-term potentiation in type I adenylyl cyclase mutant mice. Neuron 1998;20:1199–1210. [PubMed: 9655507]

Tang WJ, Krupinski J, Gilman AG. Expression and characterization of calmodulin-activated (type I) adenylyl cyclase. J Biol Chem 1991;266:8595–8603. [PubMed: 2022671]

Tzavara ET, Pouille Y, Defer N, Hanoune J. Diurnal variation of the adenylyl cyclase type 1 in the rat pineal gland. Proc Natl Acad Sci U S A 1996;93:11208–11212. [PubMed: 8855334]

Villacres EC, Wong ST, Chavkin C, Storm DR. Type I adenylyl cyclase mutant mice have impaired mossy fiber long-term potentiation. J Neurosci 1998;18:3186–3194. [PubMed: 9547227]

Villacres EC, Wu Z, Hua W, Nielsen MD, Watters JJ, Yan C, Beavo J, Storm DR. Developmentally expressed Ca(2+)-sensitive adenylyl cyclase activity is disrupted in the brains of type I adenylyl cyclase mutant mice. J Biol Chem 1995;270:14352–14357. [PubMed: 7782295]

Wang H, Pineda VV, Chan GC, Wong ST, Muglia LJ, Storm DR. Type 8 adenylyl cyclase is targeted to excitatory synapses and required for mossy fiber long-term potentiation. J Neurosci 2003;23:9710–9718. [PubMed: 14585998]

Welker E, Armstrong-James M, Bronchti G, Ourednik W, Gheorghita-Baechler F, Dubois R, Guernsey DL, Van der Loos H, Neumann PE. Altered sensory processing in the somatosensory cortex of the mouse mutant barrelless. Science 1996;271:1864–1867. [PubMed: 8596955]

Wong ST, Athos J, Figueroa XA, Pineda VV, Schaefer ML, Chavkin CC, Muglia LJ, Storm DR. Calcium-stimulated adenylyl cyclase activity is critical for hippocampus-dependent long-term memory and late phase LTP. Neuron 1999;23:787–798. [PubMed: 10482244]

Xia Z, Choi EJ, Wang F, Blazynski C, Storm DR. Type I calmodulin-sensitive adenylyl cyclase is neural specific. J Neurochem 1993;60:305–311. [PubMed: 8417150]

Xia ZG, Refsdal CD, Merchant KM, Dorsa DM, Storm DR. Distribution of mRNA for the calmodulin-sensitive adenylate cyclase in rat brain: expression in areas associated with learning and memory. Neuron 1991;6:431–443. [PubMed: 2001286]

Zalutsky RA, Nicoll RA. Comparison of two forms of long-term potentiation in single hippocampal neurons. Science 1990;248:1619–1624. [PubMed: 2114039]

The abbreviations used are

AC
: adenylyl cyclase

cAMP
: cyclic adenosine monophosphate

kD
: kilodalton

LTP
: long-term potentiation

PKA
: protein kinase A

LTD
: long-term depression

HCl
: hydrochloric acid

EDTA
: ethylenediamine tetraacetic acid

DTT
: dithiothreitol

HRP
: horseradish peroxidase

PMSF
: phenylmethanesulfonyl fluoride

SDS
sodium dodecyl sulfate

PAZ
presynaptic active zone

PSD
postsynaptic density

NR2B
NMDA receptor 2B subunit

SNAP
synaptosomal associated protein 25

NMDA
N-methyl-D-aspartic acid

SEM
standard error of the mean

DAPI
4’,6 diamidino-2-phenylindole

MAP-2
microtubule-associated protein-2

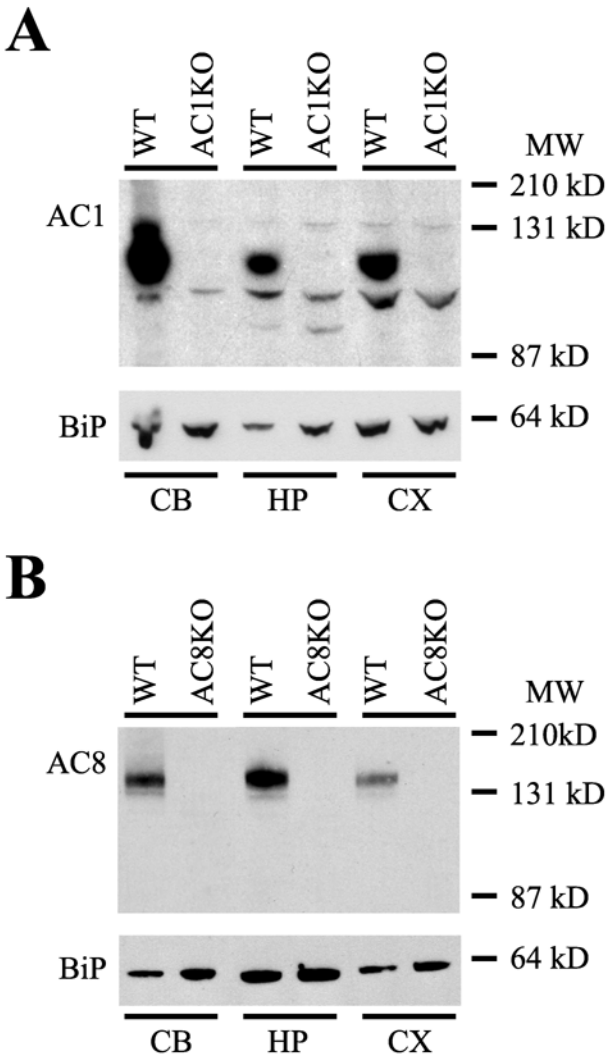

Fig 1.

Protein immunoblot analysis of AC1 and AC8 expression. Abundant protein expression of both AC1 and AC8 was detected in membrane-enriched protein extracts from the cerebellum (CB), hippocampus (HP) and cortex (CX) of the adult mouse brain. (A) A single immunoreactive band at ~123 kD, representing AC1 protein was detected in all WT but not AC1KO samples. (B) A single immunoreactive band at ~135 kD, representing AC8 protein was detected in all WT but not AC8KO samples. Equal loading conditions were verified by immunodetection for binding protein (BiP). MW, Molecular weight.

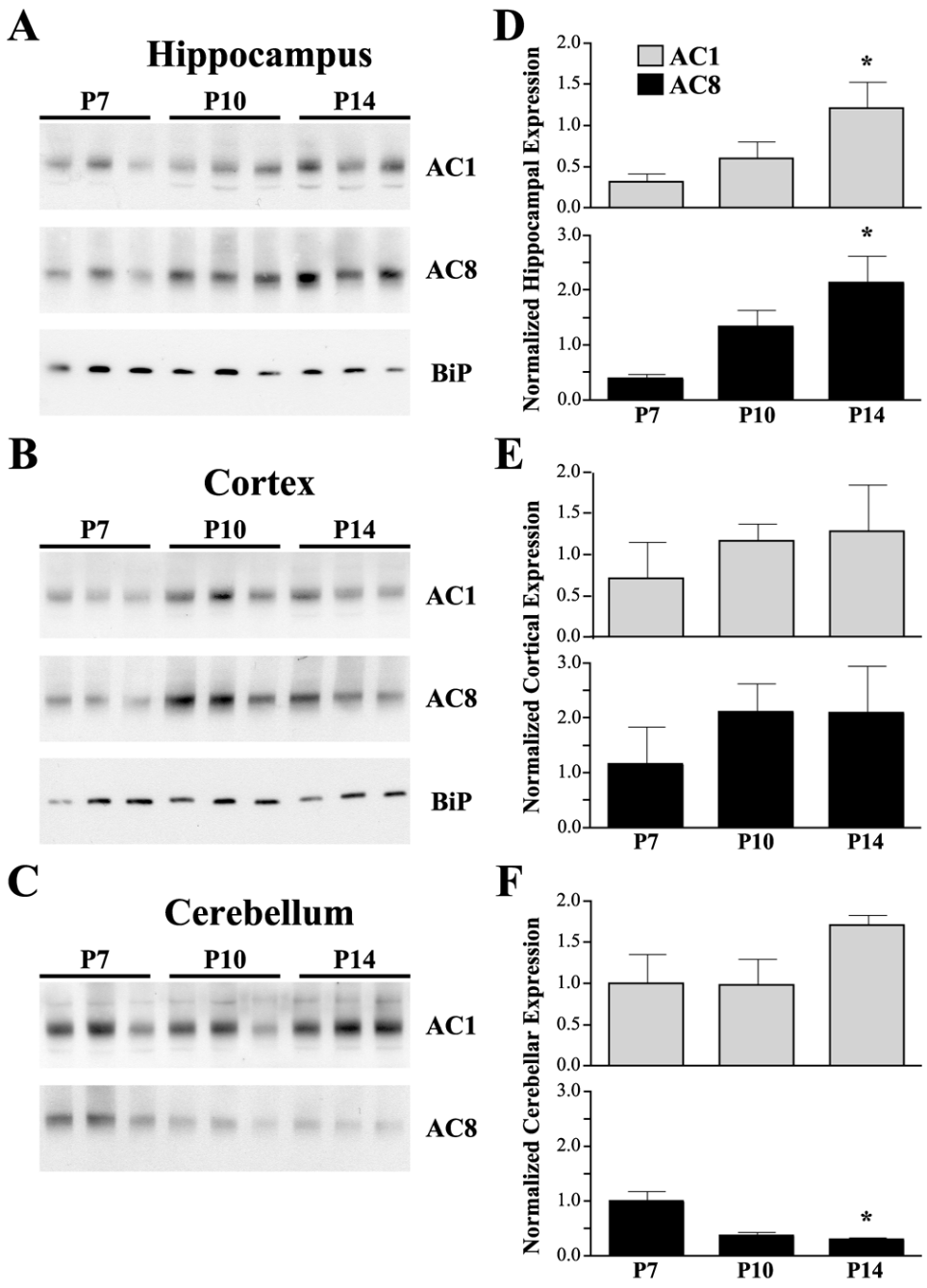

Fig 2.

Protein immunoblot analysis and quantification of developmental expression of AC1 and AC8 in WT mice. (A) Increasing expression of AC1 and AC8 was detected in the hippocampus from P7 to P14. (B) Cortical expression of both AC1 and AC8 demonstrated an increasing trend from P7 to P14. (C) AC1 protein expression did not increase significantly in the cerebellum from P7 to P14 while expression of AC8 protein significantly decreased from P7 to P14. Normalized intensity of AC1 and AC8 immunoreactivity in (D) hippocampal, (E) cortical and (F) cerebellar extracts from WT mice (n=3/timepoint). Values expressed as average +/− SEM. MW, Molecular weight. *, $p < 0.05$ vs. P7

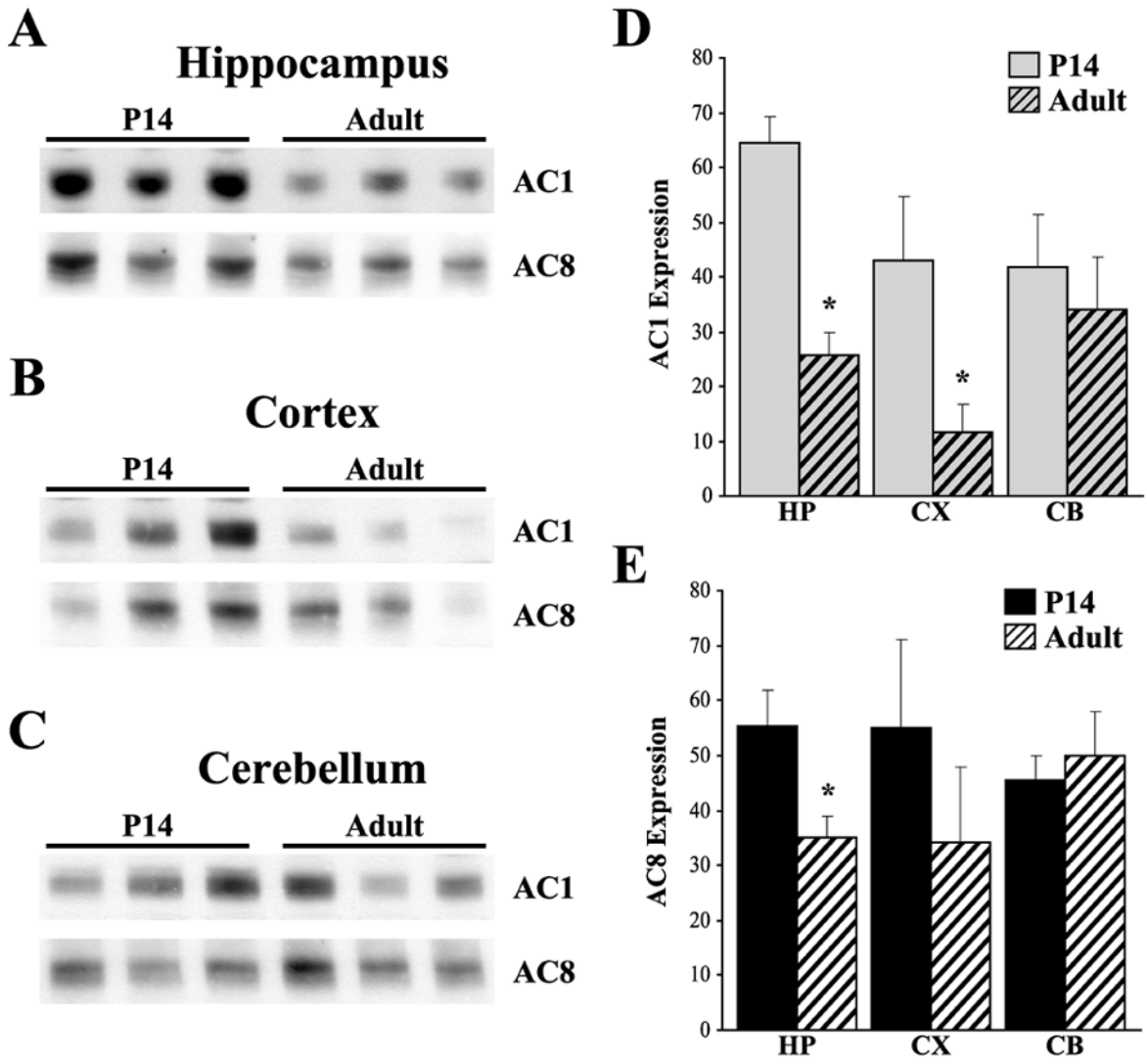

Fig 3.

Protein immunoblot analysis and quantification of developmental expression of AC1 and AC8 in WT mice. (A) Decreased expression of AC1 and AC8 was detected in the hippocampus from P14 to adulthood. (B) Decreased expression of AC1 was detected in the cortex from P14 to adulthood, with a trend towards decreased expression of AC8 by adulthood. (C) In contrast, expression of both AC1 and AC8 remain unchanged with age after P14 in the cerebellum. Abundance of AC1 (D) and AC8 (E) immunoreactivity in hippocampal (HP), cortical (CX) and cerebellar (CB) extracts from WT mice (n=3/timepoint). Values expressed as average +/− SEM. MW, Molecular weight. *, $p < 0.05$ vs. P14

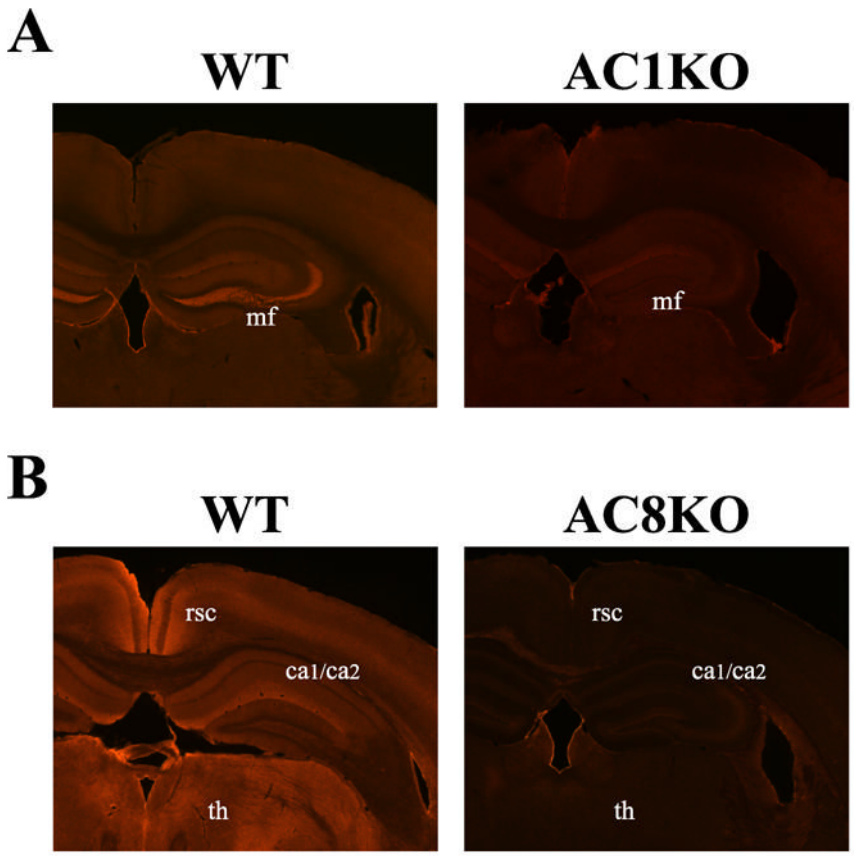

Fig 4.

Localization of AC1 and AC8 protein in the mouse brain by immunohistochemistry. Representative coronal sections at 200X magnification from the adult mouse brain demonstrate unique patterns of protein distribution of AC1 and AC8. (A) AC1 immunoreactivity was robustly expressed in mossy fiber (mf) projections from the dentate hilus region extending to the stratum lucidum of the CA3 region of the hippocampus, with diffuse expression in the cortex and thalamus in the WT mouse. AC1 immunoreactivity is not detected in AC1KO mice demonstrating specific antigen recognition. (B) AC8 immunoreactivity is abundantly present in the CA1/CA2 (ca1/ca2) region in the hippocampus, habenula, retrosplenial cortex (rsc) and various thalamic nuclei (th) with weaker expression in the cerebral cortex in the WT mouse. AC8 immunoreactivity is not detected in AC8KO mice.

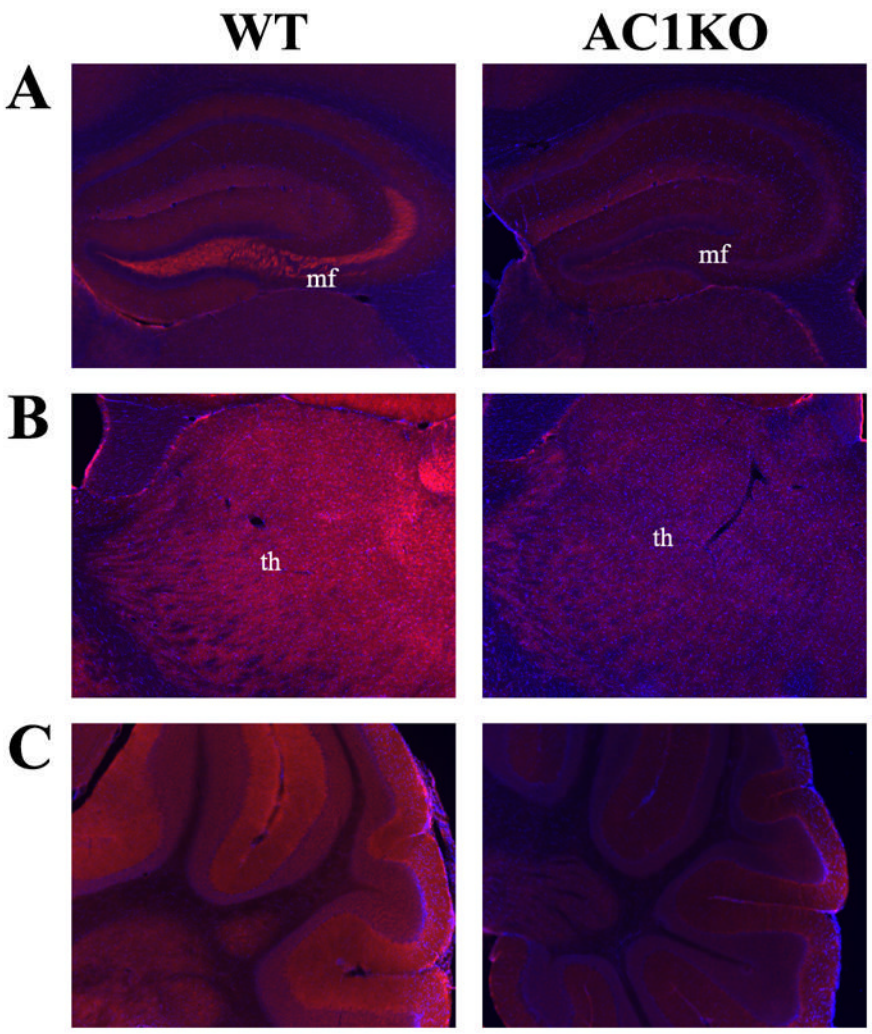

Fig 5.

Localization of AC1 protein in the adult mouse brain by immunohistochemistry. Representative (A, B) coronal and (C) sagittal sections at 400X magnification from the adult mouse brain demonstrate cellular distribution. (A) AC1 immunoreactivity was localized to the mossy fiber (mf) projections from the dentate hilus region extending to the stratum lucidum of the CA3 region of the hippocampus. AC1 was also weakly detected in the dendritic arbors of the dentate gyrus. (B) Generalized AC1 immunoreactivity was detected in the thalamus (th), without association to a particular nucleus. (C) Abundant AC1 levels were observed in the molecular layer of the adult cerebellum, which contains parallel fibers that extend from cerebellar granule cells. Sections are counterstained with DAPI (blue) to provide anatomical context.

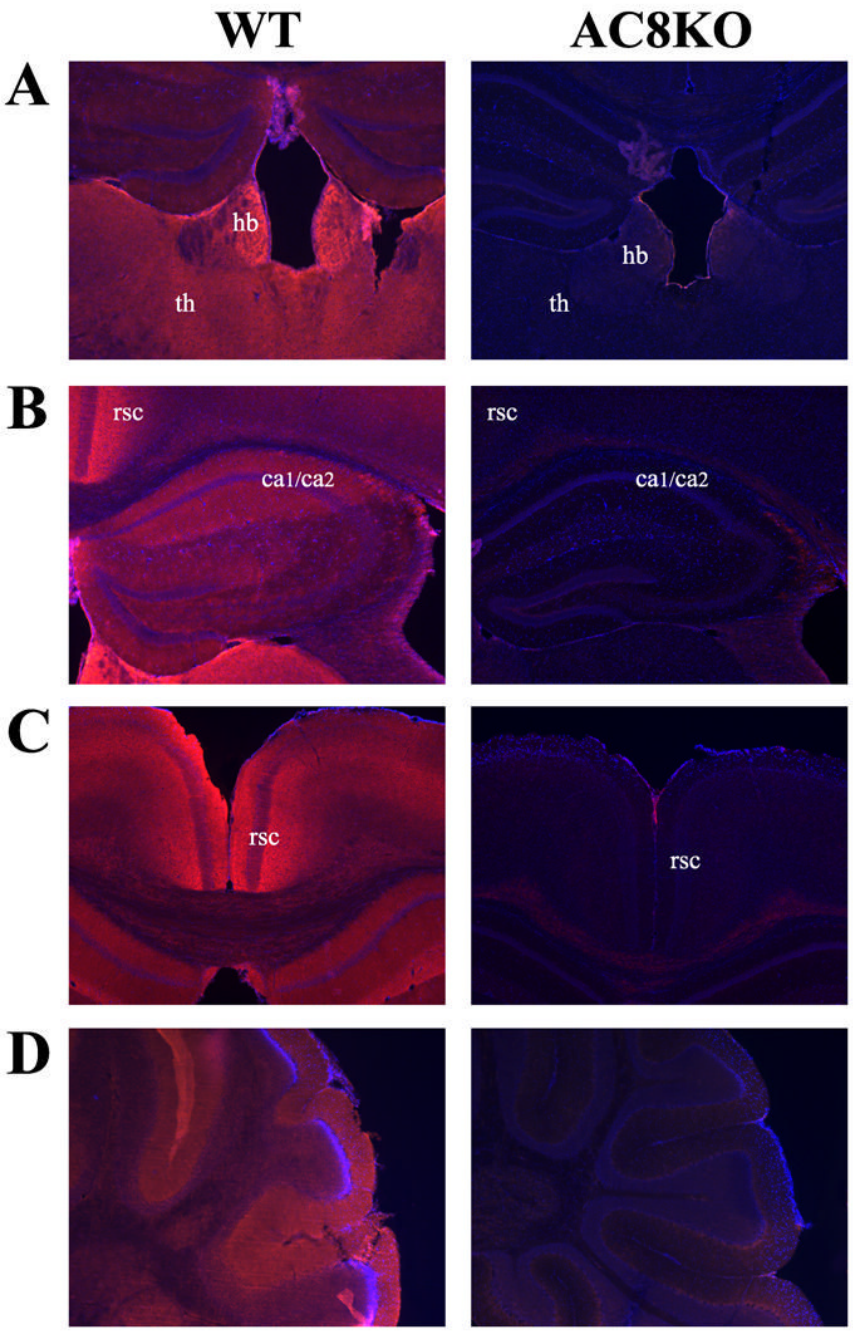

Fig 6.

Localization of AC8 protein in the adult mouse brain by immunohistochemistry. Representative (A, B, C) coronal and (D) sagittal sections at 400X magnification from the adult mouse brain demonstrate cellular distribution. (A) Intense AC8 immunoreactivity was observed in the habenula (hb) and thalamus (th). (B) AC8 was intensely localized to dendritic arbors in the oriens, molecular layer and stratum radiatum of the CA1/CA2 (ca1/ca2) region of the hippocampus. (C) Robust AC8 immunoreactivity was observed in the retrosplenial cortex (rsc), extending into intermediate cortical layers. (D) AC8 was detected in the molecular layer of the cerebellum, which contains parallel fibers extending from cerebellar granule cells. Sections are counterstained with DAPI (blue) to provide anatomical context.

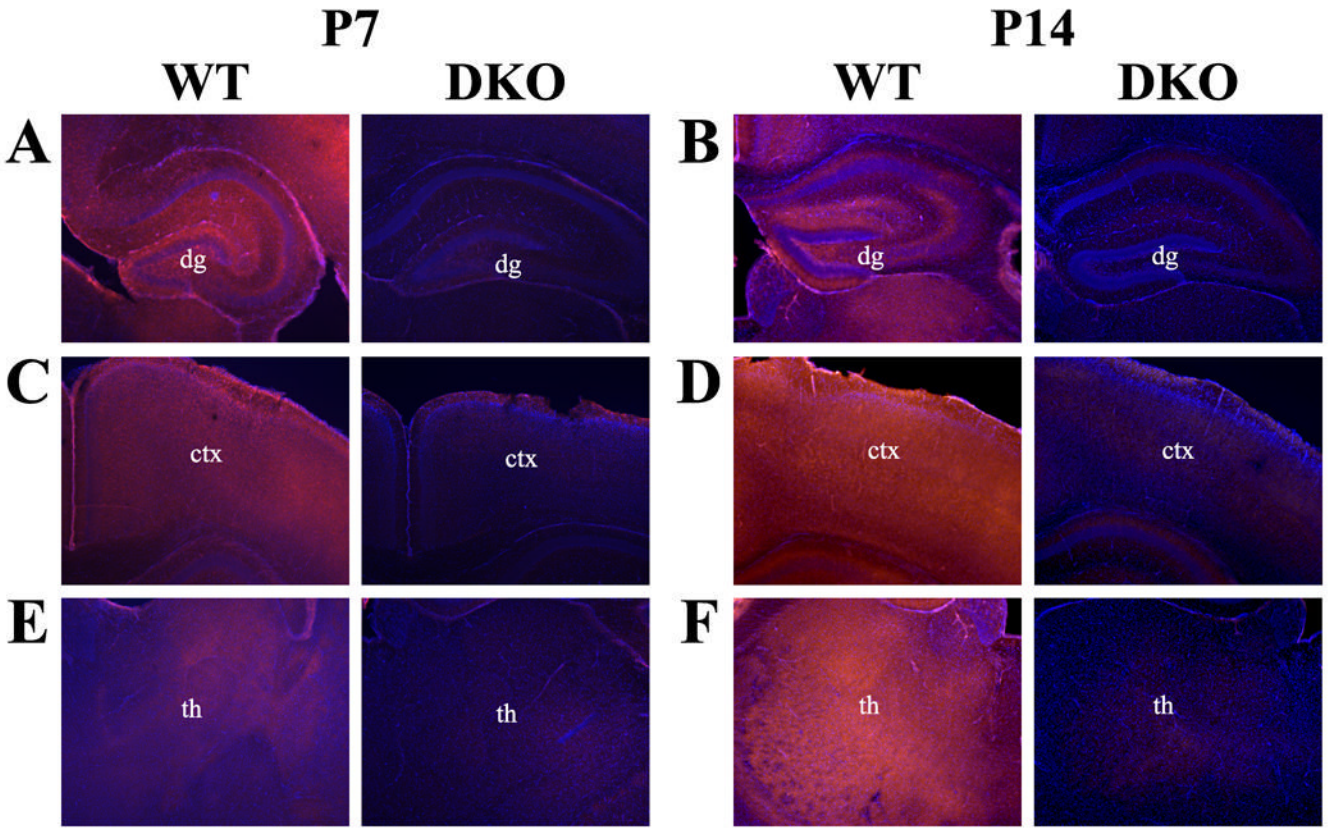

Fig 7.

Localization of AC1 protein in the developing mouse brain by immunohistochemistry. Representative coronal sections at 400X magnification from the neonatal mouse brain at postnatal day 7 (P7) and postnatal day 14 (P14) illustrate the dynamic progression of AC1 protein expression. (A) AC1 protein is widely expressed throughout the hippocampal formation at P7. (B) Expression of AC1 resembles adult expression by P14, with specific staining localized to the mossy fiber projections and the dendritic arbors of the dentate gyrus (dg). Cortical (ctx) expression of AC1 is diffuse at both (C) P7 and (D) P14, without localization to a particular cell layer. AC1 protein is expressed widely throughout various thalamic (th) nuclei at both (E) P7 and (F) P14. Sections are counterstained with DAPI (blue) to provide anatomical context.

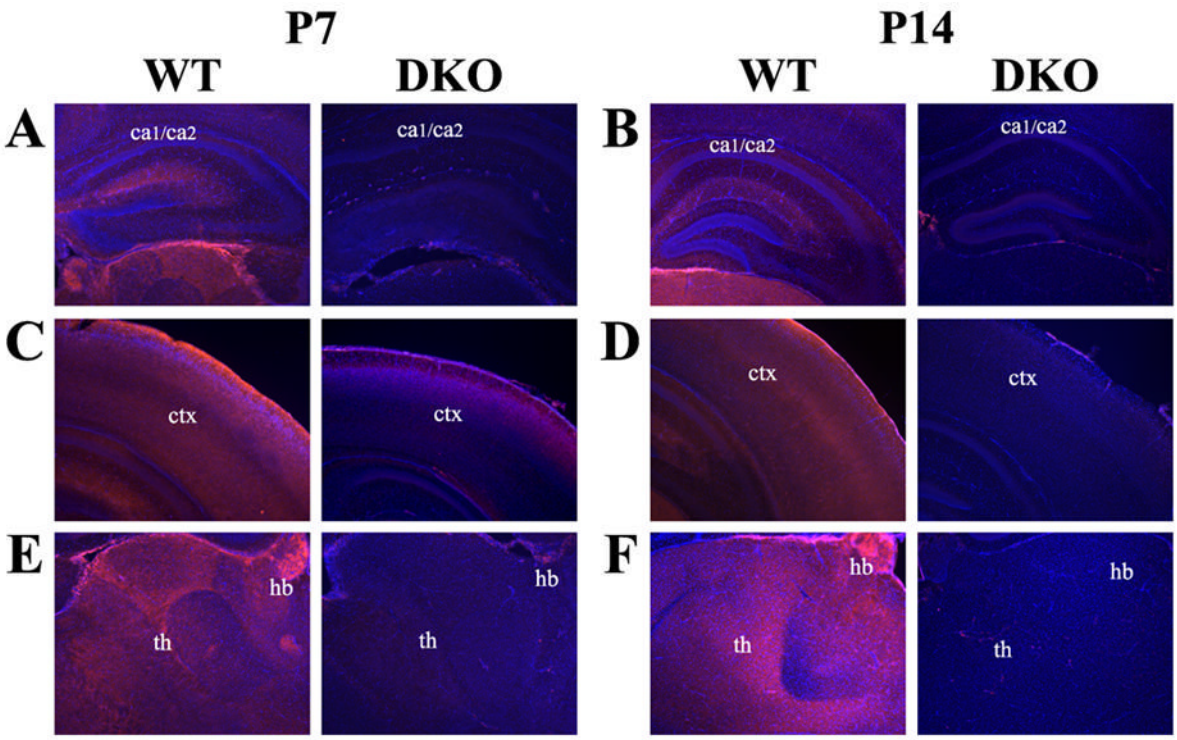

Fig 8.

Localization of AC8 protein in the developing mouse brain by immunohistochemistry. Representative coronal sections at 400X magnification from the neonatal mouse brain at postnatal day 7 (P7) and postnatal day 14 (P14) illustrate the dynamic progression of AC8 protein expression. (A) AC8 protein is weakly expressed throughout the hippocampal formation at P7. (B) Expression of AC8 increases, resembling adult expression by P14, with specific staining localized to the CA1/CA2 (ca1/ca2) regions of the hippocampus. (C) Cortical (ctx) AC8 expression is localized to deeper cortical layers at P7 becoming more intensely expressed in intermediate cortical layers by (D) P14. (E) AC8 expression in the thalamus (th) was more restricted, with robust protein levels in laterodorsal and mediodorsal thalamic nuclei as well as the habenula (hb) at P7. (F) By P14 intense AC8 staining was also observed in multiple thalamic nuclei, including the ventroposterolateral and ventromedial nuclei. Sections are counterstained with DAPI (blue) to provide anatomical context.

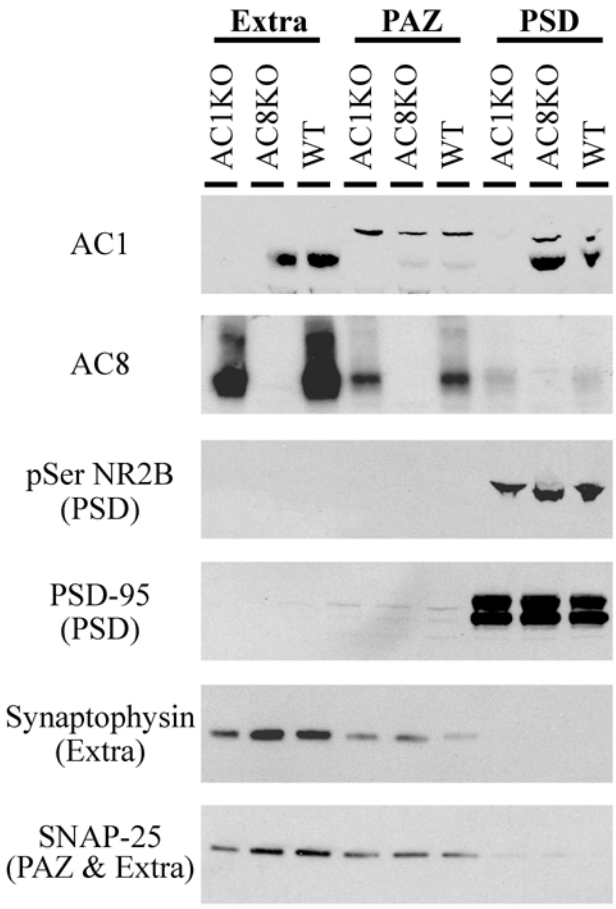

Fig 9.

Protein immunoblot analysis of AC1 and AC8 in synaptosome fractions reveals distinct patterns of subcellular distribution. Intense AC1 immunoreactivity is detected in extrasynaptic membrane (extra) and postsynaptic density (PSD) fractions, with minimal expression in the presynaptic active zone (PAZ). In contrast, AC8 is localized to extrasynaptic membrane and PAZ fractions, with minimal expression in the PSD. The extrasynaptic fraction includes both pre- and postsynaptic membranes. Appropriate enrichment of fractions is confirmed with markers of the PSD (pSer NR2B and PSD-95), the extrasynaptic pool (synaptophysin and SNAP-25), and the PAZ (SNAP-25).

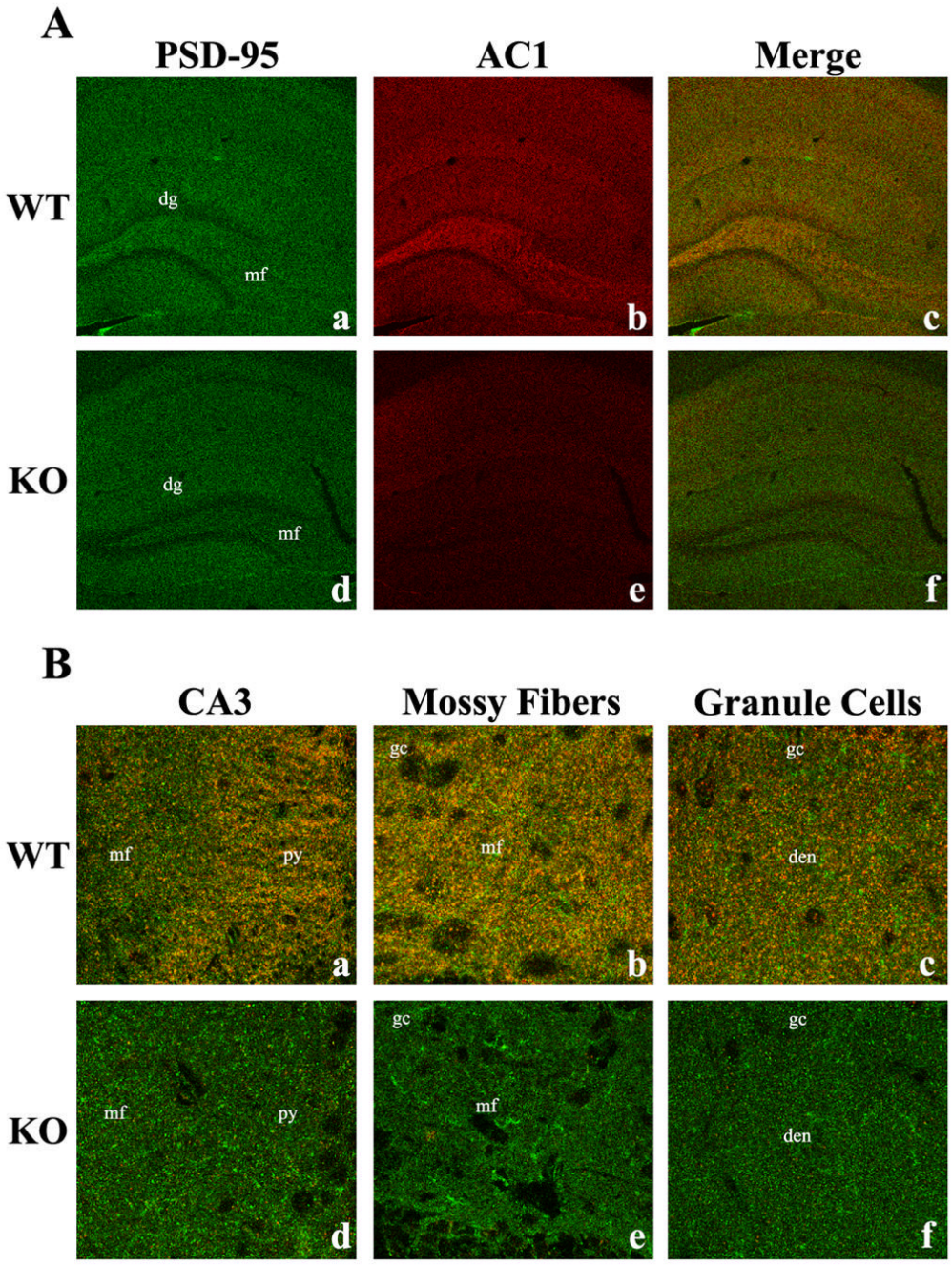

Fig 10.

Immunohistochemical co-localization of AC1 protein with PSD-95 in the adult mouse brain. A 100X confocal image of adult hippocampal sections demonstrates the specificity of the postsynaptic protein, PSD-95 (green, Aa), and AC1 (red, Ab) and their co-localization (yellow, Ac), indicating the association of AC1 with postsynaptic proteins. In contrast, mice lacking both AC1 and AC8 exhibit only PSD-95 immunoreactivity (Ad, Ae, Af). Further analysis at 900X demonstrates the co-localization of PSD-95 and AC1 in hippocampal substructures such as the mossy fiber (mf)/CA3 pyramidal cell (py) junction (Ba), the proximal mossy fiber pathway in the dentate hilus (Bb) and the dendritic arbors of the dentate granule cells (Bc). dg, dentate gyrus; gc, dentate granule cells; den, dendrites.

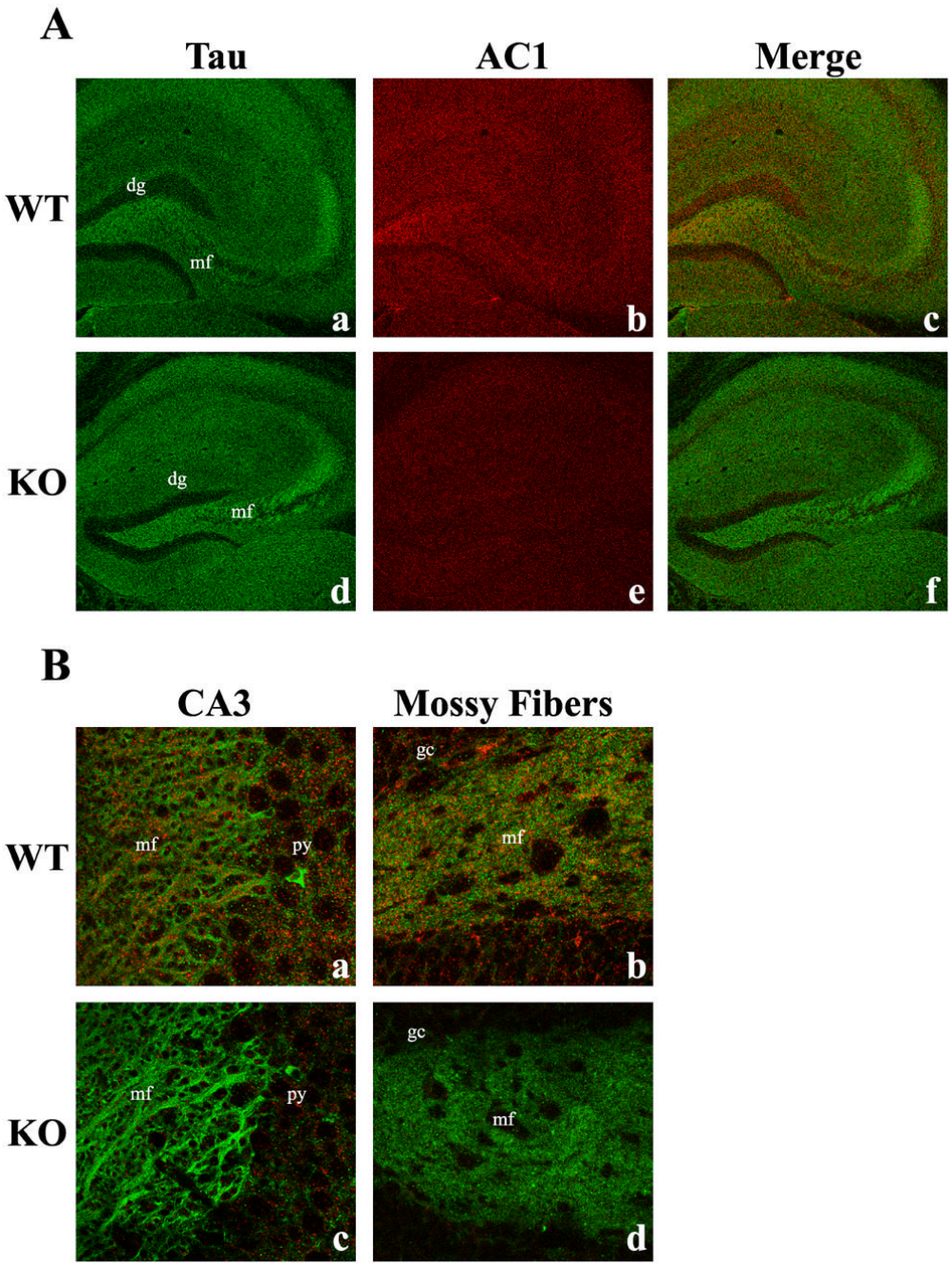

Fig 11.

Immunohistochemical co-localization of AC1 protein with Tau in the adult mouse brain. A 100X confocal image of adult hippocampal sections demonstrates the specificity of the microtubule protein (extrasynaptic), Tau (green, Aa), and AC1 (red, Ab) and their co-localization (yellow, Ac), indicating the association of AC1 with extrasynaptic axonal proteins. In contrast, mice lacking both AC1 and AC8 exhibit only Tau immunoreactivity (Ad, Ae, Af). Further analysis at 900X demonstrates the co-localization of Tau and AC1 in hippocampal substructures such as the mossy fiber (mf)/CA3 pyramidal cell (py) junction (Ba) and the proximal mossy fiber pathway in the dentate hilus (Bb). dg, dentate gyrus; gc, dentate granule cells.

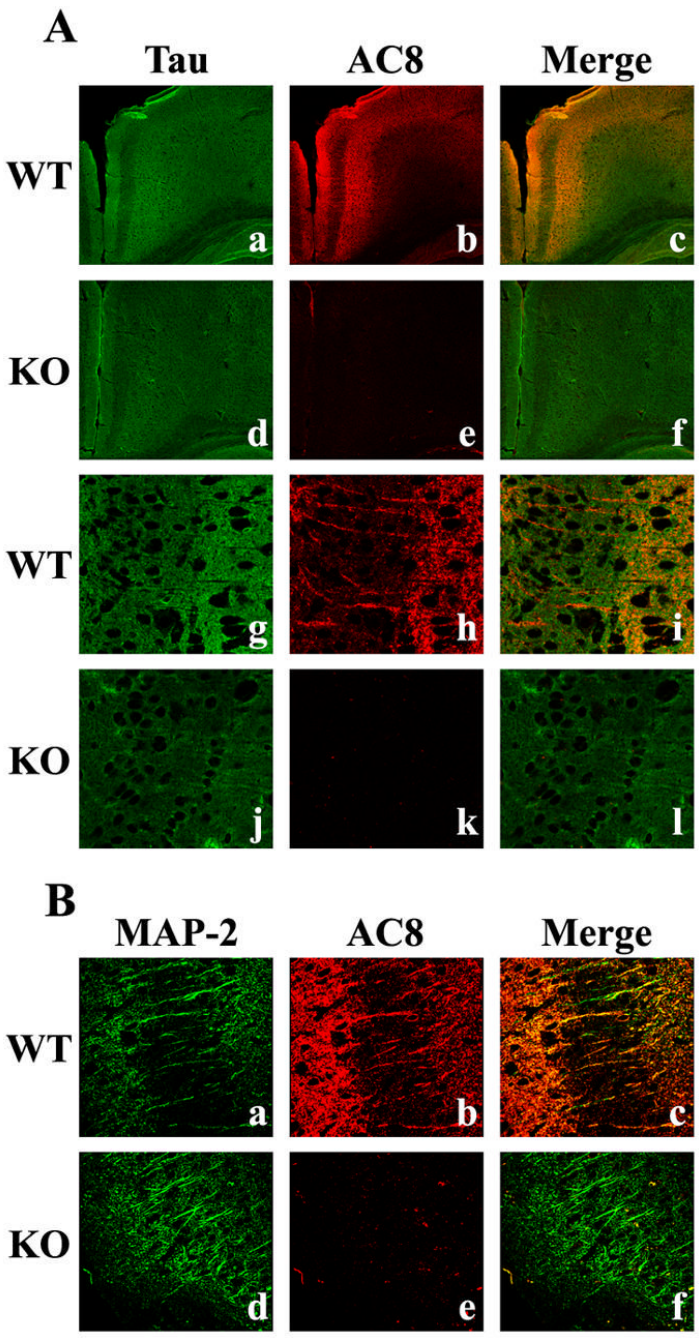

Fig 12.

Immunohistochemical co-localization of AC8 protein with Tau and MAP-2 in the adult mouse brain. A 100X confocal image of adult cingulate cortex sections demonstrates the specificity of the microtubule protein (extrasynaptic), Tau (green, Aa), and AC8 (red, Ab) and their co-localization (yellow, Ac), indicating the association of AC8 with extrasynaptic axonal proteins. In contrast, mice lacking both AC1 and AC8 exhibit only Tau immunoreactivity (Ad, Ae, Af). Analysis at 900X further demonstrates the co-localization of Tau (Ag) and AC8 (Ah) in extrasynaptic structures within the cingulate (Ai) of WT mice, but not in mice lacking AC1 and AC8 (Aj, Ak, Al). Confocal images at 600X magnification of the dendritic protein, MAP-2

(green, Ba), and AC8 (red, Bb) demonstrates their co-localization (yellow, Bc) within dendrites of the cingulate cortex of WT, but not AC8KO mice (Bd, Be, Bf).